Elsevier Editorial System(tm) for Marine Micropaleontology
Manuscript Draft

Manuscript Number:

Title: Zinc incorporation in the miliolid foraminifer Pseudotriloculina rotunda under laboratory conditions

Article Type: Research Paper

Keywords: Foraminifera; Miliolid; Zn/Ca; LA-ICP-MS; culture experiments; pollution.

Corresponding Author: Dr. Maria Pia Nardelli,

Corresponding Author's Institution: University of Angers

First Author: Maria Pia Nardelli

Order of Authors: Maria Pia Nardelli; Daniele Malferrari; Annalisa Ferretti; Annachiara Bartolini; Anna Sabbatini; Alessandra Negri

Abstract: The incorporation rate of Zn into the calcareous tests of Pseudotriloculina rotunda was investigated in culture in order to evaluate the possibility to use Zn/Ca ratios as pollution proxy. Foraminifera were incubated at zinc concentrations up to 10-fold higher than unpolluted seawater (sea+10 mg Zn/L) during 70 days. New calcite was observed at Environmental Scanning Electron Microscopy (ESEM), for potential alteration of test structure. Laser ablation-Inductively Coupled Plasma-Mass spectrometer (LA-ICP-MS) was used to quantify Zn contents. The analyses revealed that test structure is not visibly altered by the presence of zinc. However, significant Zn incorporation is detected by LA-ICP-MS. The zinc partition coefficient, DZn, decreases at increasing Zn concentrations (from 4.03±0.06 at control conditions to 0.2±0.01 at the highest tested Zn concentration) and the zinc is incorporation into the calcite follows a power function.

Zinc incorporation in the miliolid foraminifer *Pseudotriloculina rotunda* under laboratory conditions

Nardelli M.P.[1,2,*], Malferrari D.[3], Ferretti A.[3], Bartolini A.[4], Sabbatini A.[1], Negri A.[1]

[1] Department of Life and Environmental Sciences (DiSVA), Politechnic University of Marche, Ancona, Italy

[2] Present address: UMR CNRS 6112 LPG-BIAF, University of Angers, Angers, France

[3] Department of Chemical and Geological Sciences, University of Modena and Reggio Emilia, Modena, Italy

[4] Centre de Recherche sur la Paléobiodiversité et les Paléoenvironnements, UMR 7207 CNRS MNHN UPMC, Muséum National d'Histoire Naturelle, Paris Cedex 05, France

*corresponding author: Maria Pia Nardelli, UMR CNRS 6112 LPG-BIAF, University of Angers, 2 Boulevard Lavoisier, 49045 Angers Cedex, France. Email: mariapia.nardelli@univ-angers.fr Telephone: +33241735390

Highlights

1- Zinc incorporation into miliolid foraminiferal tests was experimentally tested; 2- *Pseudotriloculina rotunda* was cultured at several zinc concentrations for 70 days; 3- LA-ICP-MS analyses show that Zn is incorporated into calcite; 4- Partition coefficients (D_{Zn}) decrease at increasing $Zn/Ca_{seawater}$ ratios.

ABSTRACT

The incorporation rate of Zn into the calcareous tests of *Pseudotriloculina rotunda* was investigated in culture in order to evaluate the possibility of using Zn/Ca ratios as a pollution proxy. Foraminifera were incubated at zinc concentrations up to 10-fold higher than unpolluted seawater (sea+10 mg Zn/L) during 70 days. New calcite was investigated under Environmental Scanning Electron Microscope (ESEM), for potential alteration of test structure. Laser ablation-Inductively Coupled Plasma-Mass spectrometry (LA-ICP-MS) was used to quantify Zn contents. The analyses revealed that test structure is not visibly altered by the presence of zinc. However, significant Zn incorporation is detected by the LA-ICP-MS. The zinc partition coefficient, D_{Zn}, decreases at increasing Zn concentrations (from 4.03±0.06 to 0.2±0.01) and the zinc is incorporated into the calcite, non-necessarily linearly.

KEYWORDS

Foraminifera; Miliolid; Zn/Ca; LA-ICP-MS; culture experiments; pollution.

1. Introduction

The recent worldwide legislation aims to restore the “pre-anthropic impacts” status in marine environments (e.g., WFD, 2000/60/EC and MSFD, 2008/56/EC in Europe). Information about the pristine faunas like those in pre-industrial times, however, are often impossible to obtain because of the scarcity (or lack) of reference stations that could still represent unimpacted present-day

conditions. Fossilizing organisms represent an excellent historical archive of environmental conditions. Foraminifera are distributed worldwide in many different habitats, from brackish to marine, and their fossil records create an excellent historical archive which can be used as proxies for the reconstruction of past environments, such as pre-industrial ecological conditions (Schönfeld et al. 2012). A new approach involves the use of foraminiferal test geochemistry to assess the evolution of pollutant (i.e., metals) concentrations through time. Incorporation rates of trace elements are widely used as specific proxies in paleoceanography and paleoecology (e.g., Eggins et al. 2003; Hönisch and Hemming 2005; Levi et al. 2007; Katz et al. 2010; Sabbatini et al. 2011), despite the possible bias linked to the biological influence on calcification processes (i.e., vital effects). The need to calibrate these proxies through culturing experiments was highlighted in the last decade by several authors (e.g., de Nooijer et al. 2007). This approach offers the advantage of changing one single variable (while all the others are kept constant) in order to better evaluate the vital effect. These biological aspects could be even more important for the incorporation rates of chemicals whose concentrations exceed natural baselines due to human activity, and that could be potentially used as pollution markers.

In this study we investigate the incorporation rates of Zn in the shell of the benthic miliolid foraminifer *Pseudotriloculina rotunda* (Schlumberger 1893). Among foraminiferal species miliolids showed contradictory responses to heavy metal pollution in different studies. For example, decreasing miliolid relative abundances in polluted (by both organic and inorganic chemicals) coastal zones are reported and interpreted by some authors as a sensitivity index (e.g., Ferraro et al. 2006; Frontalini and Coccioni 2008). Other studies, on the other hand, suggest a strong tolerance of several miliolid species to pollution, both *in situ* and under laboratory conditions (e.g., Samir and El-Din 2001; Romano et al. 2008; Cherchi et al. 2009; Foster et al. 2012; Nardelli et al. 2013).

The aim of the present study is to calibrate incorporation rates of Zn in miliolid foraminiferal shells and thus evaluate the usefulness of the Zn incorporation rate as an environmental proxy. Zn is, in fact, one of the most common pollutants associated with human activities (e.g., Callender and Rice

2000; Wuana and Okieimen 2011), that can be toxic for biological systems when its concentration exceeds a threshold value (e.g., Haase et al. 2001; Valko et al. 2005; Díaz et al. 2006; Formigari et al. 2007). Nardelli et al. (2013) showed that inorganic Zn at concentrations higher than 0.1 mg/L can cause biological stress in *Pseudotriloculina rotunda*, causing delay in calcification rates.

In this regard, our study also aims to test the hypothesis that the biological stress caused by high Zn concentrations may influence metal incorporation rates as well. Zn incorporation was investigated using the Laser Ablation Inductively Coupled Plasma Mass Spectrometer (LA-ICP-MS) analysis. Moreover, morphological observation using the Environmental Scanning Electron Microscope (ESEM) was employed to check for abnormalities in the organization/distribution of single shell crystallites. Nardelli et al. (2013) previously suggested that Zn does not cause macroscopic test deformations in miliolid foraminiferal shells, on the base of their observation of coiling patterns and chamber shapes of *P. rotunda* specimens grown at increasing zinc concentrations, under the binocular microscope. The aim of our ESEM analyses was to deepen these observations and check for calcite anomalies at the crystallite level.

2. Material and Methods

2.1 Experimental set up

All the analyses were performed on specimens of *Pseudotriloculina rotunda* that grew at least one chamber during 70-days exposure to six different Zn concentrations under laboratory conditions. Zn-enriched solutions were prepared adding respectively 0.01, 0.1, 1.0, 10, and 100 mg/L of Zn to natural seawater (sea) from an unpolluted site (Portonovo, Adriatic Sea); Zn and Ca concentrations in natural seawater were measured using Inductively Coupled Plasma Mass Spectrometer (ICP-MS). Although precautions were taken during manipulations, the ICP-MS analyses revealed that the zinc concentration of the natural seawater used for the experiment was higher than natural background. In fact the zinc concentration measured on culture waters before the addition of zinc was 0.149±0.01 mg/L, while the zinc concentration of seawater from the sampling site was originally of 0.237±0.01

92 µg/L. However, as the same water was used to prepare all the zinc solutions for the different
93 treatments and, considering the very high concentrations of added zinc, we believe that this
94 contamination does not compromise the dataset. But, of course, this means that the lowest tested
95 seawater zinc concentration of the experiment (named "sea" hereafter) cannot be considered as a
96 control representative of unpolluted seawater conditions.
97 Temperature (15.0±0.5°C), salinity (38.0±0.001) and pH (8.0±0.1) were kept constant during the
98 experiment. Refer to Nardelli et al. (2013) for further details on culture settings and preparation of
99 Zn solutions.
100 As reported in Nardelli et al. (2013), none of the specimens produced new chambers at the highest
101 tested Zn concentration (sea+100 mg/L), therefore only specimens coming from culture sets from
102 treatments sea, sea+0.01, sea+0.1, sea+1 and sea+10 mg/L were investigated. Moreover, two
103 samples were treated for a "passive Zn incorporation test": empty tests of *P. rotunda* were exposed
104 to sea+10 mg/L Zn concentrations for two weeks in order to measure Zn passively adsorbed to
105 calcite, without involving cellular-mediated mineralization processes.
106

107 *2.2 ESEM and LA-ICP-MS sample preparation*
108 The analyzed foraminiferal tests (n=41) were washed with millipore water and dried at 40°C. The
109 same cleaning procedure was performed on the two empty tests (n=2) used for the passive
110 incorporation test. To perform both ESEM observations and LA-ICP-MS analyses, samples were fixed
111 to aluminium stubs using conductive carbon adhesive discs. All samples analysed with an LA-ICP-MS
112 were photographed under the ESEM before and after the analyses to check for the success of
113 ablations (i.e., the correct chamber, no multiple chamber sampling, and no breakage of chambers –
114 see Appendix, Figs. A.1a-c).
115

116 *2.3 LA-ICP MS analysis: analytical protocol optimization*

This study represents the first LA-ICP-MS investigation on miliolid foraminifera. Chemical composition, micro-structure and chamber arrangements of miliolids strongly differ from other benthic foraminifera more commonly analyzed with the LA-ICP-MS (i.e., Rotaliidae, e.g., de Nooijer et al. 2007; Munsel et al. 2010; Dissard et al. 2010; or Buliminidae, e.g., Hintz et al. 2006; Barras et al. 2010). Miliolid foraminifera have a calcareous non-lamellar imperforate test consisting of calcite needles randomly oriented in an organic matrix. They also possess a smoothly finished outermost layer of well crystallized calcite, with rhombohedral crystal faces arranged parallel to the surface (Debenay et al. 1998). Moreover, *Pseudotriloculina rotunda* creates chambers, each one-half coil in length, adding the new ones in planes oriented at 120°, with only three final externally visible chambers (Loeblich and Tappan 1964).

For this reason it was necessary to optimize the existing protocols and to obtain the best ablation setting to be applied to our specimens. In particular, it was compulsory to prevent the laser from ablating the innermost (older) chambers. Several trials on foraminiferal tests were thus performed to find the most suitable combination of the instrument setting parameters. A detailed description of the followed procedures is given in Appendix A, and the values of the optimized parameter used for measurements are reported in Table 1. An example of successful sampling is shown in Figure 1.

2.3.1 Analytical standards preparation and instrument calibration

A mass spectrometer, like any measurement device, requires a suitable calibration procedure. When laser ablation is employed, the interaction between laser and solid sample is complex and the response is dependent on the sample matrix. For this reason, two forms of calibration are mandatory: i) a reference (internal standard) is required to compensate for changes in the quantity of ablated mass, even when the concentration remains constant; ii) matrix-matched solid standards (frequently referred to as “external standards”) are necessary to calibrate laser ablation processes and the instrument response. In fact, a relative measure of ablated mass can be achieved by simultaneously measuring emission from the analyte and a common matrix element (internal

143 standard). For absolute calibration of the LA-ICP-MS conditions, standards made of the same matrix
144 as the samples would be required, but are seldom available (e.g., Darke and Tyson 1994; Raith et al.
145 1996; Hathorne et al. 2003).
146 Previous studies on perforate calcareous species of foraminifera (or other organisms with calcareous
147 compounds) used NIST610-611 or NIST612-613 as external standards, together with internal
148 standards (generally ^{44}Ca isotope) and "in-house made standards" (e.g., Hathorne et al. 2003; Eggins
149 et al. 2003; Montagna et al. 2007; Rathmann and Kuhnert 2008; Munsel et al. 2010). The same
150 standards were also used in our study in order to test their possible employment also for miliolids.
151 In-house made standards were obtained as hereafter described. Stock solutions with defined Zn
152 concentration were prepared using Zn ICP-standard solutions [1mg/mL in 2 (vol.%) HNO_3] and
153 Millipore water. A proper amount of each solution was added to a mixture composed by 400 mg of
154 ultrapure $CaCO_3$ powder (particle size less than 1 micron) and cellulose; to prevent $CaCO_3$ dissolution,
155 the pH of each solution was adjusted to 7.5± 0.1 using an appropriate amount of ammonia solution.
156 Each suspension was mixed and homogenized in an agate mortar and then dried at 30°C for 12
157 hours. The resulting powder was then re-homogenized in the agate mortar and pressed at 12 tons
158 into tablets of 12 mm diameter. Such "standard tablets" at different Zn concentrations were then
159 checked via LA-ICP-MS using ablation lines to verify whether Zn distribution was homogeneous. As
160 shown in Figure 2, the spectra resulting from these analyses revealed a fairly smooth plateau,
161 confirming a homogeneous distribution of the element into the standard tablets.
162 According to the literature (see above), NIST standards could be used as well. However, the
163 difference in composition of the matrix (i.e., silica glass in NIST standards, Ca carbonate in miliolids)
164 does not match the second requirement mentioned above. However, several measurements using
165 NIST610 were performed in order to test the possibility to use a certified and easily acquired
166 analytical standard. In particular, the same laser parameters (i.e., the same ablation conditions) were
167 applied to both NIST610 and our samples (miliolids) but the response on the internal standard (^{44}Ca)
168 was not satisfactory (see next paragraph for more details).

In the light of these results, and also in agreement with Hathorne et al. (2003), only in house-made Tablets were used as external standards for measurements here reported. In detail, nine in house made standards were used with Zn concentrations ranging from 0 (blank, $CaCO_3$+cellulose+Millipore) to 1050 ppm.

2.4 LA-ICP-MS: analyses of samples and data elaboration

Eleven specimens from "sea", five from sea+0.01 mg/L, six from sea+0.10 mg/L, ten from sea+1.0 mg/L, nine from sea+10 mg/L, were analyzed by the LA-ICP-MS. Moreover, the two specimens for the "passive sorption tests" were investigated as well. In few cases more than one ICP-MS analysis was carried out on the same chamber, otherwise one linear ablation per chamber was generally realized. Standards were ablated using exactly the same laser setting parameters used for foraminifera, and their concentrations were regularly measured during sampling procedure, in order to correct instrumental deviation.

^{66}Zn and ^{68}Zn isotopes, and ^{44}Ca were measured. A mix of helium (95%) and hydrogen (5%) were used as reaction gas and a collision and reaction cell (KED) was used to minimize spectral interferences. Both for calibration and for sample measurements, Ca and Zn concentrations were calculated integrating over a time-interval of 1.00E+05ms in the flattest region of each spectrum of each individual ablation profile using PlasmaLab^{TM} Software Package 2007.

For data analyses the relation between Zn/Ca ratios in calcite and seawater was observed. Partition coefficients for Zn were calculated for each set of Zn enriched cultures following the formula D_{Zn}= $(Zn/Ca)_{calcite}/(Zn/Ca)_{seawater}$.

3. Results

3.1 ESEM observations

193 Results from ESEM observations on structure and crystal organization of Zn-exposed foraminiferal
194 tests did not reveal any obvious anomalies. All specimens showed the typical structure of miliolid
195 tests (Figs. 3 a-d), characterized by organized crystals on the external test surface and disorganized
196 crystals in an organic matrix in the inner part of the wall (Hay et al. 1963; Towe and Cifelli 1967;
197 Haake 1971; Debenay et al. 1998).
198 ESEM observations were also performed to adjust laser ablation parameters (see Appendix A) and to
199 check samples for correct ablation after LA-ICP-MS measurements.
200

201 *3.2 LA-ICP-MS measurements*

202 The main results of the LA-ICP-MS analysis are given in Figure 4 (a,b). The Zn seawater concentrations
203 are given in Zn/Ca mmol/mol to facilitate the comparison with Zn/Ca ratios in the calcite. The
204 different treatments (i.e., Zn concentrations) are indicated by the colors. The LA-ICP-MS analysis
205 revealed that Zn/Ca ratio increases linearly with water concentrations at least up to sea+1.0 mg/L
206 (Fig. 4b). The Zn/Ca shell concentrations vary between 1.11±0.02 mmol/mol for the "sea" treatment
207 and 1.77±0.04 mmol/mol of the treatment sea+1.0 mg/L (Tab. 2; see also Tab. A.2 in Appendix A for
208 the complete dataset). The measurements obtained on calcite produced at the highest tested Zn
209 concentrations (sea+10 mg/L), however, with average Zn/Ca values of 3.81±0.17 mmol/mol, suggest
210 the possibility that the linear trend, observed for seawater Zn concentrations lower than sea+1.0
211 mg/L, can turn towards a plateau for higher concentrations. Possible explanations of this trend are
212 discussed later.
213 The passive sorption test on empty shells incubated at sea+10 mg/L conditions showed very low Zn
214 concentrations ($Zn/Ca_{calcite}$= 1.17±0.01 mmol/mol), comparable to the ones of samples from the
215 "sea" treatment) ($Zn/Ca_{calcite}$=1.12±0.02 mmol/mol), and more than 3 times lower than living samples
216 from highest tested zinc concentrations (sea+10 mg/L) ($Zn/Ca_{calcite}$=3.83±0.17 mmol/mol) (Fig. 4 and
217 Tab. A.2 of Appendix A).

The calculated Zn partition coefficients (D_{Zn}) for each Zn treatment (indicated by the colors) are given in Figure 5a. The average D_{Zn} (±standard deviation) is given in numbers. Because of inhomogeneous variance, the Kruskal-Wallis test and Mann-Whitney pairwise comparisons post-hoc test were performed to determine whether the difference between partition coefficients was significant among treatments (p-value < 0.001). The results showed that the Zn partition coefficients were all significantly different among treatments. The obtained average values of D_{Zn} varied between 4.03±0.06 at "sea" conditions and 0.2±0.01 at sea+10 mg/l Zn concentration (Fig. 5) (total average D_{Zn}= 2.22±1.56). The observed decrease of D_{Zn} at increasing seawater Zn concentration is well described by a power function (R^2=0.997; p-value<0.001; see Fig. 5a). However, due to the difficulty to assess whether the results obtained for the highest tested concentration (sea+10 mg/L) are real or affected by neglected precipitation of zinc oxides/hydroxides (see discussion paragraph 4.2) we reported in fig. 5b only the D_{Zn} obtained at Zn treatments lower than this concentration. Even without the last concentration, the data are still well described by a power function (R^2=0.998; p-value<0.001) and the regression equation slightly change from $y= 1.5552x^{-0.713}$ to $y = 1.4826x^{-0.775}$.

4. Discussion

4.1 ESEM structural observation of tests

Miliolids are often regarded as pollution sensitive organisms. Several studies on test deformity induced by environmental contamination suggest that miliolids are more easily affected by test deformities than other foraminifera. For example, Samir and El-Din (2001) found that the majority of deformed tests collected in the El-Mex Bay (Egypt) were miliolid shells. Also Sharifi et al. (1991) reported that deformed foraminiferal tests from the Southampton coastal area contained much higher Cu and Zn concentrations than non-deformed specimens, suggesting again a responsibility of these metals for test deformations. However, Nardelli et al. (2013) tested in laboratory conditions the biological effects of several Zn concentrations on *P. rotunda* and, despite the fact that some

specimens calcified new chambers at Zn concentrations up to 10 mg/L, no obvious deformations due to Zn exposure were observed, in terms of chamber arrangements or general shape of the foraminiferal shells. Our ESEM observations confirm these results because the calcite produced during Zn exposure showed the typical aspect and arrangement known for the species (as described by Debenay et al. 1998). Then, Zn exposure does not appear to be, by itself, a cause of abnormal calcification for *P. rotunda*, either at the macro or micro scale. A possible explanation for the fact that Zn is often found in anomalous tests is its possible covariance with other pollutants (for example other metals) or environmental parameters, which can be alone the real cause of test deformation or have synergic behaviors to zinc and enhance its toxicity (as demonstrated, for example, for Co and Zn by Bresson et al. 2013). In fact, even if Zn is one of the most cited heavy metals, potentially responsible for test deformation, many other pollutants and anthropogenic events were related to test deformities, e.g. Cd, Cr and Ti (Yanko et al. 1998), Cu (Le Cadre and Debenay 2006), hydrocarbons and oil spills (e.g., Vénec-Peyré 1981; Vénec-Peyré et al. 2010), rapid changes of salinity and hypersalinity (e.g., Eichler-Coelho et al. 1996; Sousa et al. 1997; Stouff et al. 1999; Geslin et al. 2002). The absence of visible test anomalies can be coherent with the hypothesis that Zn incorporation into biomineralized calcite may occur, as already observed on non-biogenic calcites (e.g., Elzinga and Reeder 2000; Temmam et al. 2000), after substitution of Ca or Mg to form isomorphic Zn carbonates, as suggested by Madkour and Ali (2009).

4.2 Zinc incorporation

Despite the absence of deformations or visible abnormalities in the specimens analyzed in this study, high Zn/Ca contents were detected in the internal wall of the last chamber of the test by LA-ICP-MS analysis. The incorporation rates of Zn into the calcite do not seem to be constant at increasing Zn concentrations. Zn incorporation, in fact, linearly increases at lower concentrations (from sea to sea+1.0 mg/L, Fig. 4b), but the measures obtained at Zn concentrations higher than sea+1.0 mg/L, even if represented by the results from only one Zn treatment, suggest that at higher concentrations

(i.e., sea+10 mg/L) the trend determined at low concentrations (up to sea+1.0 mg/L) is no longer respected (Fig. 4a). The decreasing Zn incorporation rate in the shell is reflected by the partition coefficients that are lower for higher Zn seawater treatments (Fig. 5a,b).

Considering that we worked at high zinc concentrations we cannot avoid to take into account that zinc oxides/hydroxides precipitation could have been important at the highest zinc concentration we tested (sea+10 mg/L). In fact, if we roughly estimate the expected Zn^{2+} saturation based on the pH of our cultures (8.0±0.1) and neglect all potential influences of kinetics, we obtain a concentration of saturation of 4.37E-05 M, which is 3 times lower than the concentration of zinc we added to this treatment (see Tab. A.2 in Appendix A). Zinc oxides/hydroxides precipitation could therefore at least partially explain the decrease of Zn incorporation at sea+10 mg/L condition.

However, this is not the first time that a similar decreasing trend for metal incorporation is observed on benthic foraminifera and this could be also partially due to biological reasons. For example Munsel et al. (2010) report similar observations for incorporated Ni in *A. tepida*'s calcite. The incorporation of the metal is linear at low experimental concentrations and drops down when foraminifera are exposed to Ni concentrations 20-fold higher than natural seawater. The authors suggest that this could be due to biological effects. In fact, according to them, Ni at high concentrations could have toxic effects on foraminiferal cells and inhibit calcification. Toxic potential of some highly concentrated metals could trigger their cellular expulsion or blocking mechanism (for example metallothioneins-mediated) and prevent their incorporation in proportion to their sea water concentrations. This hypothesis is also valid for our study. Nardelli et al. (2013) reported delayed growth rates (i.e. calcification) of *Pseudotriloculina rotunda* exposed to Zn concentrations higher than sea+1.0 mg/l and ascribed the reduced calcification rate to biological effects of high zinc concentrations on foraminiferal cell, invoking similar processes. Thus we think that the potential biological influence on the Zn incorporation observed at sea+10 mg/l in the present study cannot be excluded. Some other possible explanations are hypothesized by Mewes et al. (2014) who also observed an exponential decreasing partition coefficient for Mg/Ca at increasing seawater metal

concentrations following a power regression for two rotaliid foraminifera (*Ammonia aomoriensis* and *Amphistegina lessonii*): (a) presence of two different $CaCO_3$ layers, (b) involvement of two different biomineralization pathways. The first hypothesis depends on the possibility, shown for some foraminifera, to precipitate two different calcite phases, with two different Mg/Ca calcite ratios, independently of a migration of the foraminifera through different chemical environments (in the water column or in the sediment). This pathway was described by Bentov and Erez (2005) and particularly for *A. lessonii and Orbulina universa* by Branson et al. (2013). However, as far as we know, this biomineralization mechanism has not been described and does not fit with the existing calcification models for miliolid foraminifera. In fact the existing biomineralization models for miliolid foraminifera propose two kinds of calcification mechanisms: some miliolid foraminifera form bundles composed of an array of oriented crystals. Each crystal is enveloped by organic material, and then bundles are passed through the cell membrane by exocytosis. Other miliolids, instead, accrete pre-formed crystals and matrix materials onto extracellular surfaces to form a loosely packed wall structure in a "stack-of-bricks" process (e.g., Berthold 1976; Hemleben et al. 1986).

The second hypothesis considers the involvement of different biomineralization pathways of Mg incorporation during calcification. This hypothesis derives from the biomineralization model proposed by Nehrke et al. (2013) for rotaliids foraminifera, but there is no evidence that the same processes occur into miliolid foraminifera. Therefore also this hypothesis does not seem to be valid to explain our results. Thus, the oversaturation of the highest tested zinc solution and/or the biological effect of potentially toxic zinc concentrations on the biomineralization process remain, to us, the more realistic hypothesis to explain the low zinc incorporation at sea+10 mg/L treatment.

A part from the exponential decrease of partition coefficient, another interesting point highlighted by our results is the apparent positive intercept of D_{Zn} ($Zn/Ca_{calcite}$ vs $Zn/Ca_{seawater}$) regression (Fig. 4b). This result suggests a difference in Zn incorporation for this miliolid species compared to all the rotaliid foraminifera for which D_{Zn} was previously estimated (e.g. Marchitto et al., 2000; Bryan and Marchitto, 2010). In fact, despite the highly variable D_{Zn} estimated for the different species,

Marchitto et al. (2000) and Bryan and Marchitto (2010), report a $Zn/Ca_{calcite}$ vs $Zn/Ca_{seawater}$ regression line passing from the origin of the axes for all the measured rotaliids foraminifera. Similar results, showing a positive intercept on the y-axis, reported in Mewes et al. (2014) for Mg/Ca of two rotaliid foraminifera (*Ammonia aomoriensis* and *Amphistegina lessonii*), were hypothesized by the authors to be possibly due to purely chemical reasons: sorption of Mg^{2+} to mineral surfaces would be stronger than sorption of Ca^{2+} (Mucci and Morse 1983) and then increased Mg^{2+} (adsorbed on calcite) would locally increase Mg/Ca, and then explain the positive y-axis intercept, especially at low seawater Mg/Ca. Due to its divalent nature and its ionic radii smaller than Ca^{2+}, this kind of mechanism is also possible for Zn^{2+} (Elzinga and Reeder, 2000). In this regard, the results of our sorption test (fig. 4) seems to suggest that, at least at the highest tested concentration (sea+10 mg/L), Zn sorption is negligible compared to the fraction incorporated into the calcite of living foraminifera incubated at the same Zn concentrations. This suggests that this kind of mechanism could have low influence on Zn enrichment of calcite. However, the test was performed only at the highest Zn treatment and it is not enough to draw any definitive conclusion about this aspect.

Another hypothesis, invoked by Langer et al. (2006) to explain the enriched Sr/Ca ratio in the calcite of the coccolithophore *Emiliania huxleyi*, could also explain the Zn/Ca enrichment we observe for *Pseudotriloculina rotunda*. Similarly to miliolid foraminifera, coccolithophores precipitate calcite into specific intracellular vesicles. According to the authors, the intracellular calcite precipitation yields an accumulation of Sr in the coccolith vesicle until Sr steady state is achieved. Then, the observed Sr/Ca of the coccolith calcite would be an integral value that arises from the sum of Sr/Ca over the time required for the formation of one coccolith. This is suggested to explain the enriched Sr/Ca ratios found into the coccolithophore compared to theorical ones expected by purely chemical precipitation. According to us, and keeping into account the results of our sorption test, this hypothesis seems more convincing to explain the apparent positive y-axis intercept of figure 4.

4.3 Implications for reconstructing past seawater zinc concentrations

As zinc is one of the most diffused pollutants related to the industrial activity (e.g., Callender and Rice 2000; Wuana and Okieimen 2011) a proxy for its concentrations in historical times could represent an important tool to study the evolution of marine ecosystems under anthropic stress. This is particularly interesting in view of the animated debates on the possible boundary for the recently proposed new epoch of the Anthropocene (e.g., Crutzen 2002; Zalasiewicz et al. 2011). The accelerated increase of some industrial-derived pollutants is, in fact, one of the proposed points to establish the start of this epoch. Our results suggest a possible reliable identification and interpretation of one of these pollutants in the historical sediment record. In fact, except for the D_{Zn} estimated for the sea+10 mg/L that could have been influenced by Zn oversaturation problems (as discussed above), we are confident that the D_{Zn} estimated for *Pseudotriloculina rotunda* in this study can be applied for past seawater concentrations reconstructions. The partition coefficients we obtained are different from the ones previously estimated for other foraminiferal species (mainly Rotaliids), but rely on the variability range of values found for different species of rotaliid foraminifera (e.g. ~3 for *U. peregrina* to ~22 for *C. pachyderma* reported by Bryan and Marchitto, 2010) and they represent the Zn/Ca of the seawater where the calcite was biomineralized. Zn/Ca contents into miliolid calcite could therefore allow reconstruction of concentrations of this metal in the past seawater.

The obtained D_{Zn} for each tested zinc concentrations (fig. 5a) show statistically significant differences. For this reason we would suggest not to average all the values but rather using the equations given in figure 4b and 5b for Zn seawater reconstructions. For the highest tested zinc concentration, for which the estimated D_{Zn} could have been highly driven by zinc oxides/hydroxides precipitation and physiological cell problems due to potential toxic effects of zinc, our results are more difficult to apply and need further investigation to be confirmed. For the use of this proxy in potentially contaminated environments, the possible toxic effect of Zn at high concentrations on *P. rotunda* could be an important boundary constraint. A possible solution to overcome this problem could be the use of multiple species, with different thresholds of tolerance to zinc.

5. Concluding remarks

Zn/Ca ratios in calcite of *Pseudotriloculina rotunda* are linear function of Zn/Ca in seawater at lower Zn/Ca seawater and appear to turn into a power function at Zn seawater concentrations higher than sea+1.0 mg/L. Further studies are needed to quantify the possible influence of zinc oxides/hydroxides precipitation on the results we obtained at this higher experimental condition. However, even if we omit the last point from the dataset, the results show that Zn is incorporated in equilibrium with seawater concentrations and that partition coefficients significantly decrease at increasing seawater zinc concentrations following a power function. The result of passive sorption test performed on dead specimens incubated in water with high Zn concentration suggests that most of the zinc incorporation is mediated by the cell and that chemical passive sorption is putatively negligible (Tab. A.2). These results suggest the suitability of Zn/Ca into foraminiferal calcite as an environmental proxy. Zinc contents of calcite can be in fact considered representative of the concentrations in seawater at the time of their calcification, and relatively independent of post-mortem conditions occurring in the depositional area. The analysis of Zn/Ca contents into the calcite could therefore allow the reconstruction of past zinc concentrations in seawater. Then, present-day knowledge about tolerance limits of foraminifera (e.g., de Freita Prazeres et al. 2011; Nardelli et al. 2013) and other organisms to Zn seawater concentrations would allow us to study potential ecological effects induced by high concentrations of this metal in environmental systems in the past. However further studies would be needed for a more precise calibration of Zn/Ca as a proxy. In particular the study of potential synergic, additive or antagonistic effects of several chemicals and/or of environmental variables (e.g., salinity, temperature, alkalinity..) on Zn incorporation should be deeply investigated. Moreover, further calibration will be very useful in the future to fill the gap for concentrations between 1 and 10 mg/L and between 0.1mg/L and natural unpolluted seawater zinc concentrations (e.g., one order of magnitude lower).

399 Acknowledgements

400 The authors thank the reviewers, G.J. Reichart and an anonymous one for their important remarks
401 and encouraging comments that strongly improved the manuscript. Thanks to the Polytechnic
402 University of Marche (Italy) for funding the research. We thank the Centro Interdipartimentale
403 Grandi Strumenti (CIGS) of the Università di Modena and Reggio Emilia (Italy) for the facilities and
404 Daniela Manzini and Maria Cecilia Rossi for the technical support. Thanks to Dr. Silvia Illuminati and
405 Prof. Scarponi for providing bottom seawater samples for background Adriatic seawater zinc
406 concentration data. Many thanks to Christine Barras and Frans Jorissen for their valuable suggestions
407 and discussions on a first draft of the manuscript.

408

409 **References**

410 Barras C., Duplessy J. C., Geslin E., Michel E., Jorissen F., 2010. Calibration of δ 18 O of laboratory
411 cultured deep-sea benthic foraminiferal shells in function of temperature. Biogeosciences 7: 1,
412 1349-1356.

413 Bentov S., Erez J., 2005. Novel observations on biomineralization processes in foraminifera and
414 implications for Mg/Ca ratio in the shells. Geology 33: 841-844.

415 Berthold W.U., 1976. Biomineralisation bei milioliden Foraminiferen und die Matrizen-Hypothese.
416 Naturwischenschaften 63:196.

417 Branson O., Redfern S.A., Tyliszczak T., Sadekov A., Langer G., Kimoto K., Elderfield H., 2013. The
418 coordination of Mg in foraminiferal calcite. Earth Planet. Sci. Lett. 383: 134-141.

419 Bresson C., Darolles C., Carmona A., Gautier C., Sage N., Roudeau S., Ortega R., Ansoborlo E., Malard
420 V., 2013. Cobalt chloride speciation, mechanisms of cytotoxicity on human pulmonary cells, and
421 synergistic toxicity with zinc. Metallomics 5: 133-143.

422 Bryan S.P., Marchitto T., 2010. Testing the utility of paleonutrient proxies Cd/Ca and Zn/Ca in benthic
423 foraminifera from thermocline waters. Geochem. Geophys. Geosystems 11: Q01005.

424 Callender E., Rice K. C., 2000. The urban environmental gradient: anthropogenic influences on the
425 spatial and temporal distributions of lead and zinc in sediments. Environ. Sci. Technol. 34: 2, 232-
426 238.

427 Cherchi A., Da Pelo S., Ibba A., Mana D., Buosi C., Floris N., 2009. Benthic foraminifera response and
428 geochemical characterization of the coastal environment surrounding the polluted industrial area
429 of Portovesme (South-Western Sardinia, Italy). Mar. Pollut. Bull. 59: 281-296.

430 Cheng J., Vieira A., 2006. Oxidative stress disrupts internalization and endocytic trafficking of
431 transferrin in a human malignant keratinocyte line. Cell Biochem. Biophys. 45: 177-84.

432 Cohen A.L., Gaetani G.A., 2010. Ion partitioning and the geochemistry of coral skeletons: solving the
433 mystery of the vital effect. In: Ion Partitioning in Ambient Temperature Aqueous Systems: from

fundamentals to applications in climate proxies and environmental geochemistry. Stoll H., Prieto M. (eds). EMU Notes in Mineralogy, London, 10, 11: 377-397.

Crutzen P. J., 2002. Geology of mankind. Nature 415: 23.

Darke S.A., Tyson J.F., 1994. Review of solid sample introduction for plasma spectrometry and a comparison of results for laser ablation, electrothermal vaporization, and slurry nebulization. Microchem. J. 50: 310-336.

Debenay J.P., Guillou J.J., Geslin E., Lesourd M., Redois F., 1998. Processus de cristallisation de plaquettes rhomboèdriques à la surface d'un test porcelané de foraminifère actuel. GEOBIOS 31: 3, 295-302.

de Freita Prazeres M., Martins S. E., Bianchini A., 2011. Biomarkers response to zinc exposure in the symbiont-bearing foraminifer *Amphistegina lessonii* (Amphisteginidae, Foraminifera). J. Exp. Mar. Biol. Ecol. 407: 116-121.

de Nooijer L., Reichart G. J., Dueñas-Bohórquez A., Wolthers M., Ernst S., Mason P., van Der Zwaan G., 2007. Copper incorporation in foraminiferal calcite: results from culturing experiments. Biogeosciences 4: 493-504.

Díaz S., Martín-González A., Gutiérrez J. C., 2006. Evaluation of heavy metal acute toxicity and bioaccumulation in soil ciliated protozoa. Environ. Int. 32: 711-717.

Dissard D., Nehrke G., Reichart G.-J., Bijma J., 2010. The impact of salinity on the Mg/Ca and Sr/Ca ratio in the benthic foraminifera *Ammonia tepida*: results from culture experiments. Geochim. Cosmochim. Acta 74: 928-940.

Elderfield H., Bertram C.J., Erez J., 1996. A biomineralization model for the incorporation of trace elements into foraminiferal calcium carbonate. Earth Planet. Sci. Lett. 142: 409-423.

Eggins S., De Deckker P., Marshall J., 2003. Mg/Ca variation in planktonic foraminifera tests: implications for reconstructing palaeo-seawater temperature and habitat migration. Earth Planet. Sc. Lett. 212: 291-306.

459 Eichler-Coelho P.B., Duleba W., Eichler B.B., Coelho-Junior C., 1996. Determinaçao do impacto
460 ecologico do Valo Grande (Iguape, SP) a partir das associaçoes de foraminiferos e tecamebas. Rev.
461 Bras. Biol. 57: 463-477.
462 Elzinga E.J., Reeder R.J., 2000. X-ray absorption spectroscopy study of Cu2 and Zn2 adsorption
463 complexes at the calcite surface: Implications for site-specific metal incorporation preferences
464 during calcite crystal growth. Geochim. Cosmochim. Acta 66, 22: 3943-3954.
465 Ferraro L., Sprovieri M., Alberico I., Lirer F., Prevedello L., Marsella E., 2006. Benthic foraminifera and
466 heavy metals distribution: a case study from the Naples Harbour (Tyrrhenian Sea, Southern Italy).
467 Environ. Pollut. 142: 274-287.
468 Formigari A., Irato P., Santon A., 2007. Zinc, antioxidants systems and metallothioneins in metal
469 mediated-apoptosis: biochemical and cytochemical aspects. Comp. Biochem. Physiol. C 146: 443-
470 459.
471 Foster W. J., Armynot du Châtelet E., Rogerson M., 2012. Testing benthic foraminiferal distributions
472 as a contemporary quantitative approach to biomonitoring estuarine heavy metal pollution. Mar.
473 Pollut. Bull. 64: 1039-1048.
474 Frontalini F., Coccioni R., 2008. Benthic foraminifera for heavy metal pollution monitoring: A case
475 study from the central Adriatic Sea coast of Italy. Estuar. Coast. Shelf S. 76: 404-417.
476 Geslin E., Debenay J.P., Duleba W., Bonetti C., 2002. Morphological abnormalities of foraminiferal
477 tests in Brazilian environments: comparison between polluted and non-polluted areas. Mar.
478 Micropal. 45: 151-168.
479 Haake F.W., 1971. Ultrastructures of miliolid walls. J. Foramin. Res. 1: 187-189.
480 Haase H., Wätjen W., Beyersmann D., 2001. Zinc induces apoptosis that can be suppressed by
481 lanthanum in C6 rat glioma cells. J. Biol. Chem. 382: 1227-1234.
482 Hathorne E.C., Alard O., James R.H., Rogers N.W., 2003. Determination of intratest variability of trace
483 elements in foraminifera by laser ablation inductively coupled plasma-mass spectrometry.
484 Geochem. Geophys. Geosyst. 4: 12, 8408, doi: 10.1029/2003GC000539.

485 Hay W.W., Towe K.M., Wright R.C., 1963. Ultramicrostructure of some selected foraminiferal tests.
486 Micropaleontology 9: 171-175.
487 Hemleben C., Anderson O.R., Berthold W., Spindler M., 1986. Calcification and chamber formation in
488 foraminifera-a brief overview. In: Biomineralization in Lower Plants and Animals. Leadbeater BSC,
489 Riding R. (eds) Clarendon Press, Oxford, p 237-249.
490 Hintz C.J., Shaw T.J., Bernhard J.M., Chandler G.T., McCorkle D.C., Blanks J.K., 2006. Trace/minor
491 element: calcium ratios in cultured benthic foraminifera. Part II: Ontogenetic variation. Geochim.
492 Cosmochim. Acta 70: 8, 1964-1976.
493 Hönisch B., Hemming N.G., 2005. Surface ocean pH response to variations in pCO_2 through two full
494 glacial cycles. Earth Planet. Sci. Lett. 236: 305-314.
495 Katz M., Cramer B.S., Franzese A., Hönisch B., Miller K.G., Rosenthal Y., Wright J.D., 2010. Traditional
496 and emerging cheochemicla proxies in foraminifera. J. Foramin. Res. 40: 2, 165-192.
497 Langer G., Gussone N., Nehrke G., Riesbell U., Eisenhauer A., Kuhnert H., Rost B., Trimborn S., Thoms
498 S., 2006. Coccolith strontium to calcium ratios in *Emiliania huxleyi*: The dependence on seawater
499 strontium and calcium concentrations. Limnol. Oceanogr. 51: 310-320.
500 Le Cadre V., Debenay J.-P., 2006. Morphological and cytological responses of *Ammonia* (foraminifera)
501 to copper contamination: Implication for the use of foraminifera as bioindicators of pollution.
502 Environ. Pollut. 143: 304-317.
503 Levi C., Labeyrie L., Bassinot F., Guichard F., Cortijo E., Waelbroeck, Caillon N., Duprat J., de Garidel-
504 Thoron T., and Elderfield H., 2007. Low-latitude hydrological cycle and rapid climate changes
505 during the last deglaciation. Geochem. Geophys. Geosyst. 8: Q05N12,
506 doi:10.1029/2006GC001514.
507 Loeblich A.R. Jr., Tappan H., 1964. Treatise on Invertebrate Paleontology. Part C, Protista 2.
508 Sarcodinia chiefly “Thecamoebians” and Foraminiferida. The Geological Society of America and
509 The University of Kansas Press. Vol.1, pp. 510.

510 Madkour H.A., Ali M.Y., 2009. Heavy metals in the benthic foraminifera from the coastal lagoons, Red
511 Sea, Egypt: indicators of anthropogenic impact on environment (case study). Environ. Geol. 58:
512 543-553.
513 Marchitto T.M., Curry W.B., Oppo D.W., 2000. Zinc concentrations in benthic foraminifera reflect
514 seawater chemistry. Paleoceanography 15: 3, 299-306.
515 Mewes A., Langer G., de Nooijer L., Bijma J., Reichart G.J., 2014. Effect of different seawater Mg^{2+}
516 concentrations on calcification in two benthic foraminifers. Mar. Micropal. 113: 56-64.
517 Montagna P., McCulloch M., Mazzoli C., Silenzi S., Odorico R., 2007. The non-tropical coral *Cladocora*
518 *caespitosa* as the new climate archive for the Mediterranean: high-resolution (weekly) trace
519 element systematic. Quaternary Sci. Rev. 26: 441-462.
520 Mucci A., Morse J.W., 1983.The incorporation of Mg^{2+} and Sr^{2+} into calcite overgrowths: Influences of
521 growth rate and solution composition. Geochim. Cosmochim. Acta 47: 217-233.
522 Munsel D., Kramar U., Dissard D., Nehrke G., Berner Z., Bijma J., Reichart G.-J., Neumann T., 2010.
523 Heavy metal uptake in foraminiferal calcite: results of multi-element culture experiments.
524 Biogeosciences 7: 2339-2350.
525 Nardelli M.P., Sabbatini A., Negri A., 2013. Experimental chronic exposure of the foraminifer
526 *Pseudotriloculina rotunda* to zinc. Acta Protozool. 52: 193-202.
527 Nehrke G., Keul N., Langer G., de Nooijer L.J., Bijma J., Meibom A., 2013. A new model for
528 biomineralization and trace-element signatures of foraminifera tests. Biogeosciences 10: 6759-
529 6767.
530 Parry S.N., Ellis N., Li Z., Maitz P., Witting P.K., 2008. Myoglobin induces oxidative stress and
531 decreases endocytosis and monolayer permissiveness in cultured kidney epithelial cells without
532 affecting viability. Kidney Blood Press Res. 31: 16-28.
533 Raith A., Hutton R.C., Godfrey J., 1996. Quantitation methods using laser ablation ICP-MS. Part 2:
534 Evaluation of new glass standards. Fresen. J. Anal. Chem. 354: 163-168.

535 Rathmann S., Kuhnert H., 2008. Carbonate ion effect on Mg/Ca, Sr/Ca and stable isotopes on the
536 benthic foraminifera *Oridorsalis umbonatus* off Namibia. Mar. Micropal. 66: 120-133.
537 Romano E., Bergamin L., Finoia M. G., Carboni M. G., Ausili A., Gabellini M., 2008. Industrial pollution
538 at Bagnoli (Naples, Italy): benthic foraminifera as a tool in integrated programs of environmental
539 characterisation. Mar. Pollut. Bull. 56: 439-457.
540 Sabbatini A., Bassinot F., Boussetta S., Negri A., Rebaubier H., Dewilde F., Nouet J., Caillon N., Morigi
541 C., 2011. Further constraints on the diagenetic influences and salinity effect on *Globigerinoides*
542 *ruber* (white) Mg/Ca thermometry: Implications in the Mediterranean Sea. Geochem. Geophys.
543 Geosyst., 12, Q10005.
544 Samir A., El-Din A., 2001. Benthic foraminiferal assemblages and morphological abnormalities as
545 pollution proxies in two Egyptian bays. Mar. Micropaleontol. 41: 193-227.
546 Schlumberger C., 1893. Monographic des Miliolidées du Golfe de Marseille. Mémoires de la
547 Société Zoologique de France. 6: 199-224.
548 Schönfeld J., Alve E., Geslin E., Jorissen F., Korsun S., Spezzaferri S. and FOBIMO, 2012. The FOBIMO
549 (Foraminiferal BIo-MOnitoring) initiative – Towards a standardised protocol for soft-bottom
550 benthic foraminiferal monitoring studies. Mar. Micropaleontol. 94-95: 1-13.
551 Sharifi A.R., Croudace T.W., Austin R.L., 1991. Benthonic foraminiferids as pollution indicators in
552 Southampton water, Southern England, UK. J. Micropal. 10: 109-113.
553 Sousa S.H.M., Duleba W., Kfouri P., Eichler B.B., Furtado V.V., 1997. Response of foraminiferal
554 assemblages to environmental changes in the Sao Sebastiao Channel, Northern Coast of Sao Paulo
555 State, Brazil. In: The First International Conference on Application of Micropaleontology in
556 Environmental Sciences, Tel Aviv, Israel, pp. 109-110.
557 Stouff V., Debenay J.P., Lesourd M., 1999. Origin of double and multiple tests in benthic foraminifera:
558 observations in laboratory cultures. Mar. Micropal. 36: 189-204.
559 Temmam M., Paquette J., Vali H., 2000. Mn and Zn incorporation into calcite as a function of chloride
560 aqueous concentration. . Geochim. Cosmochim. Acta 64: 14, 2417-2430.

561 Towe K.M., Cifelli R., 1967. Wall ultrastructure in the calcareous foraminifera: Crystallographic
562 aspects and a model for calcification. J. Paleontol. 41: 742-762.
563 Valko M., Morris H., Cronin M.T., 2005. Metals, toxicity and oxidative stress. Curr. Med. Chem. 12:
564 1161-208.
565 Vénec-Peyré M.T., 1981. Les foraminifères et la pollution: étude de la microfaune de la cale du
566 Dourduff (embouchure de la rivière de Morlaix). Cahiers de Biologie Marine 25-33.
567 Vénec-Peyré M.T., Lipps J.H., Weber M., Bartolini A., 2010. Amoco Cadiz Oil Spill and Foraminifera
568 Thirty Years Later. FORAMS 2010 (International Symposium on Foraminifera), Abstract Volume, p.
569 193.
570 Wuana R.A., Okieimen F.E., 2011. Heavy Metals in Contaminated Soils: A Review of Sources,
571 Chemistry, Risks and Best Available Strategies for Remediation. ISRN Ecology, ID 402647.
572 Yanko V., Ahmad M., Kaminski M., 1998. Morphological deformities of benthic foraminiferal tests in
573 response to pollution by heavy metal: Implications for pollution monitoring. J. Foramin. Res. 28:
574 177-200.
575 Zalasiewicz J., Williams M., Haywood A., Ellis M., 2011. The Anthropocene: a new epoch of geological
576 time? Phil. Trans. R. Soc. A 369: 835-841.

535 **Tables**

536 Tab. 1 Optimized laser parameters. Linear ablation, carried out on the flatter part of the last chamber
537 proceeding always from the centre to the aperture of the chamber, was preferred to spot ablation.
538 See Hathorne et al. (2003) for comparison and SI-1 for further information. A pre-ablation step was
539 introduced to clean the surface from potential contaminations before data acquisition.
540

	Laser Intensity (%)	Frequency (Hz)	Ablation line width (μm)	Duration (s)	Main results
Pre-ablation	10	1	55	230	Sampling only of external chamber, without crash; good signal intensity at the detector.
Ablation	50	4	55	230	

541
542
543 Tab. 2 Mean $Zn/Ca_{seawater}$, $Zn/Ca_{calcite}$ and D_{Zn} values (±standard deviations) for each Zn treatment.

Treatment	$Zn/Ca_{seawater}$ (mmol/mol)	$Zn/Ca_{calcite}$ (mmol/mol) (± s.d.)	D_{Zn} (±s.d.)
sea (control)	0.278	1.122 (±0.028)	4.034 (±0.059)
sea+0.01 mg Zn/L	0.297	1.152 (±0.012)	3.880 (±0.042)
sea+0.1 mg Zn/L	0.465	1.216 (±0.011)	2.616 (±0.024)
sea+1.0 mg Zn/L	2.145	1.771 (±0.037)	0.826 (±0.017)
sea+10.0 mg Zn/L	18.948	3.813 (±0.171)	0.201 (±0.009)

544
545

Figures

Fig. 1 Example of successful laser sampling on last chamber of *P. rotunda*

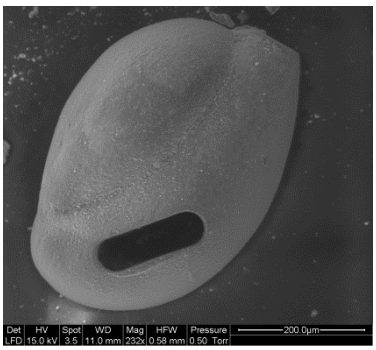

Fig. 2 Spectra resulting from the ablation lines measured on home-made standard tablets at different Zn concentrations to verify if Zn distribution was homogeneous. The highest and the lowest curves represent the spectra measured respectively on 1050 ppm and 150 ppm zinc home-made standards. CPS means counting per second.

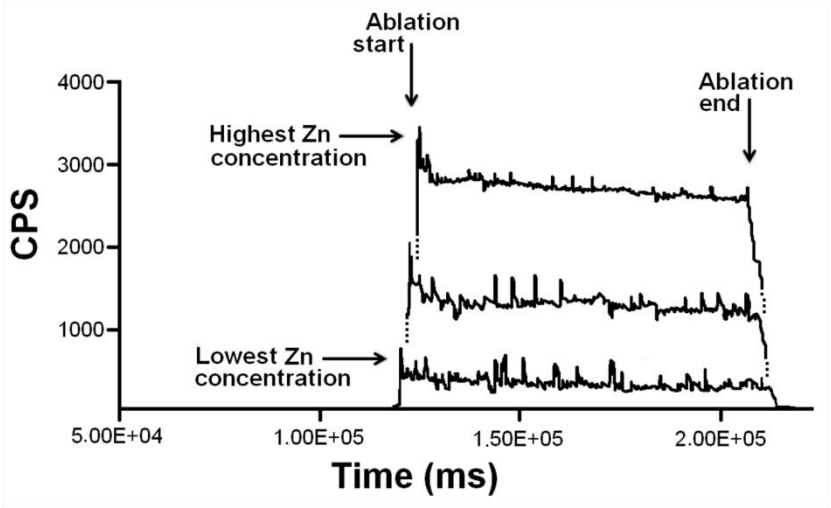

Fig. 3 ESEM micrographs of *P. rotunda*'s test. a) View of external wall of a specimen from control cultures (sea); b) detail of crystals on the external wall of the same specimen; c) View of external wall of a specimen from sea+10 mg Zn/L contaminated cultures and d) detail of internal part of the wall, with disorganized crystals of the same specimen.

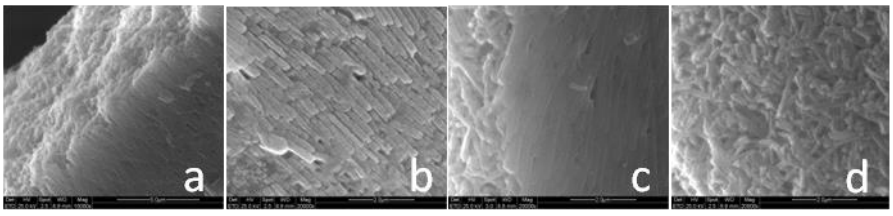

Fig. 4 Zn/Ca ratios in *Pseudotriloculina rotunda* calcite in function of Zn/Ca in seawater. a) All the samples are included (the colors correspond to the different Zn treatments). The best fitting of power function to predict $(Zn/Ca)_{calcite}$ to $(Zn/Ca)_{seawater}$ relationship is shown in blue and compared to the linear model (black dashed line). b) This is an enlargement of the left corner of figure 4a where the lower Zn/Ca points are showed separately.

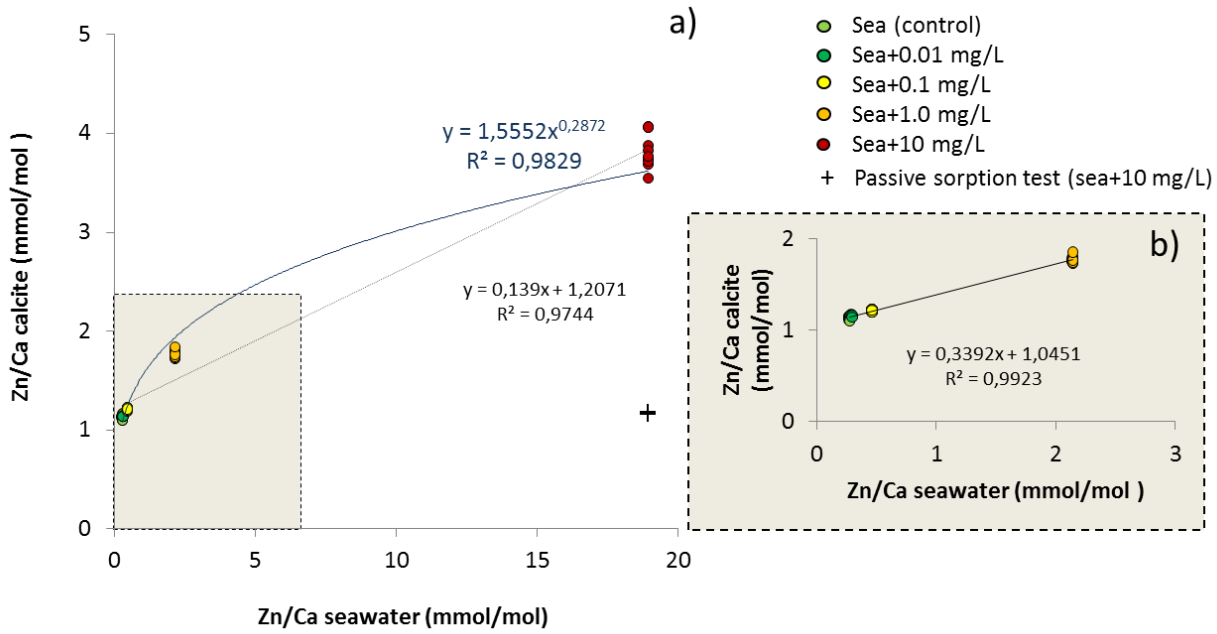

Fig. 5 Partition coefficients measured for each zinc treatment. The averages D_{Zn}± standard deviation for each treatment are given in numbers.

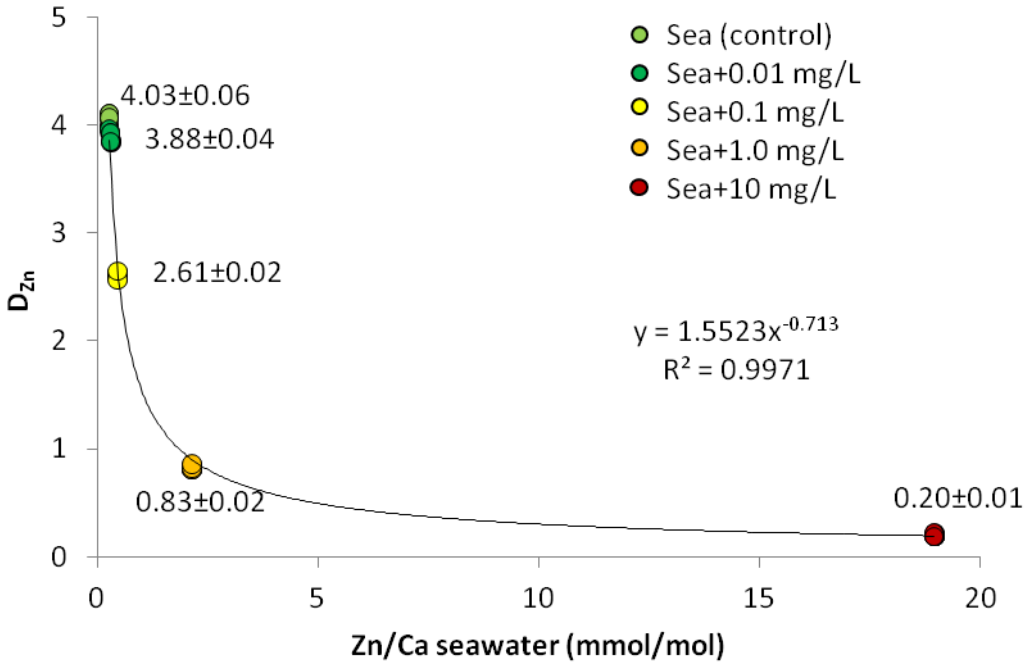

Supplementary Data for online publication only

Click here to download Supplementary Data for online publication only: Appendix A.pdf